EUROPEAN ORGANIZATION FOR NUCLEAR RESEARCH

CERN/EF 86-14
(CERN/PS 86-25 AA)
29 July 1986

DIFFERENTIATING MEASURING COILS FOR PULSED CURRENTS IN THE MA/MHz RANGE

E. Boggasch(*) and R. Grüb
CERN, Geneva, Switzerland

ABSTRACT

A precision current monitoring system was needed for a current pulse generator energizing the coaxial collector plasma lens test installation at CERN Laboratory. Based on the Rogowsky principle, a high-performance differentiating pick-up coil was designed and constructed to measure and monitor the current pulses. The layout of the pulse generator is briefly explained, followed by the description of the fundamental theory and the features of the coils. Construction details and comparative data for different types of coils are given. The main current signals are shown in the graphs. It is concluded that this new field pick-up coil is perfectly appropriate for high precision measuring equipment in the MA/MHz range.

Submitted to Review of Scientific Instruments

(*) Permanent address: Physikalisches Institut der Universität Erlangen-Nürnberg, Erwin Rommel Str. 1, D-8520 Erlangen

EF/3201F/RG/sb

1. INTRODUCTION

For many applications in physics research pulsed currents in the kA/MHz range are needed. In the framework of the plasma lens project at CERN [1], a pulse generator [2] was built to deliver peak current pulses up to 500 kA, in a repetitive mode at 0.5 Hz, into a common z-pinch load. The pulse generator consists essentially of four capacitor banks which are discharged simultaneously by four high-current pseudo-spark switches [3]. The stored energy is transferred via four strip lines to the centrally located plasma lens. The main characteristics of the current generator are listed in table 1. A simplified block diagram is shown in fig. 1.

TABLE 1 characteristics of the pulse generator

1.	Capacitance, total	108 μF
2.	Nominal charging voltage	16 kV
3.	Maximum charging voltage	20 kV
4.	Stored energy at nominal voltage	13.8 kJ
5.	Stored energy at maximum voltage	21.6 kJ
6.	Peak discharge current at nominal voltage	400 kA
7.	Peak discharge current at maximum voltage	500 kA
8.	Inductance of plasma lens	20 - 100 nH
9.	Circuit inductance	10 nH
10.	Rise time to first current maximum	1.6 μs
11.	Equivalent half sine wave length	7.4 μs
12.	Initial dI/dt at nominal current	$6 \cdot 10^{11}$ A $\cdot$ s^{-1}
13.	Voltage reversal	~ 45%
14.	Strip line cross section	540 mm x 11 mm
15.	Distance between conductors	0.9 mm
16.	Repetition period	2.4 s

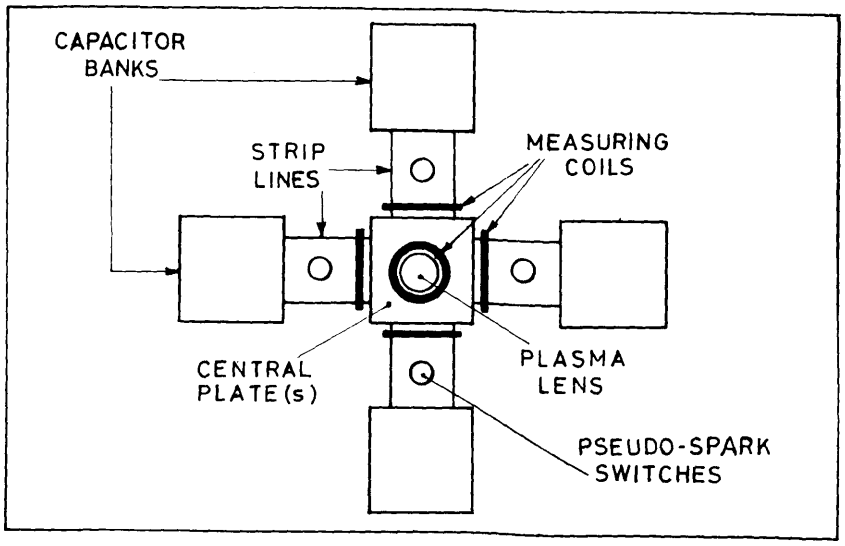

Fig. 1 Simplified block diagram of the pulse generator

Control of the switching delay time to achieve exact parallel discharge of the four banks, as well as examination of the plasma behaviour in the lens, is an essential feature of this set-up. As the plasma load presents the main inductance of the discharge circuit, plasma dynamics resulting in pinching or instabilities can be observed by the total current signal. This requires a precise high stability current monitoring system. The approximate equation describing the peak discharge current for the LRC current generator is given below

$$\hat{I} = \frac{U_o}{\sqrt{\frac{L_p}{C}}\left(\sqrt{\frac{L_p + L_c}{L_p}} + \left(\frac{\pi}{4}\sqrt{\frac{(R_p + R_c)^2 C}{L_p}}\right)\right)} , \qquad (1)$$

where U_o is the charging voltage at t_o, L_p the inductance of the plasma, L_c the remaining inductance, C the capacitance of the capacitor banks and R_c the circuit and R_p the plasma resistance. The energy transfer efficiency from the capacitor banks to the plasma lens can be expressed as

$$\eta = \frac{L_p \hat{I}^2}{C U_o^2} . \qquad (2)$$

Both R_c and L_c must therefore be kept as low as possible to minimize ohmic losses and to reach high peak currents; R_c and L_c should therefore not be increased by the measuring system.

Ohmic and/or inductive shunts are galvanically coupled to the circuit and require differential measuring at a high potential. Hall effect arrangements allow only punctual measurements at the pick-up point. Unsymmetrical current density in the 580 mm wide strip lines would falsify the results. Furthermore, a locally space-distributed current density $\underline{j}(r,\phi)$ is expected in a plasma. Other methods, such as Faraday rotation, require additional equipment.

As current measurements are required directly around the plasma volume, only pick-up coils surrounding strip line(s) and plasma could be considered. The integrated induced voltage in such coils created by the varying magnetic flux, represents a real image of the current. These considerations led to the design and construction of the differentiating measuring coils described below.

2. THEORY

The Rogowsky principle is shown in fig. 2. For a distributed current density j which is surrounded by a closed line circumscribing an area "A", neglecting displacement currents, Oersted's law is valid

$$\oint_a \underline{H} \cdot d\underline{a} = \iint_A \underline{j} \cdot d\underline{A} \ . \tag{3}$$

Integration of the right hand term leads to

$$\oint_a \underline{B} \cdot d\underline{a} = \mu\mu_o I \ , \tag{4}$$

where I is the total current penetrating "A". For a short line f, enclosing an area "F" by surrounding "a", the induction law can be expressed as follows:

$$\oint_f \underline{E} \cdot d\underline{f} = - \frac{\partial}{\partial t} \iint_F \underline{B} \cdot d\underline{F} \ . \tag{5}$$

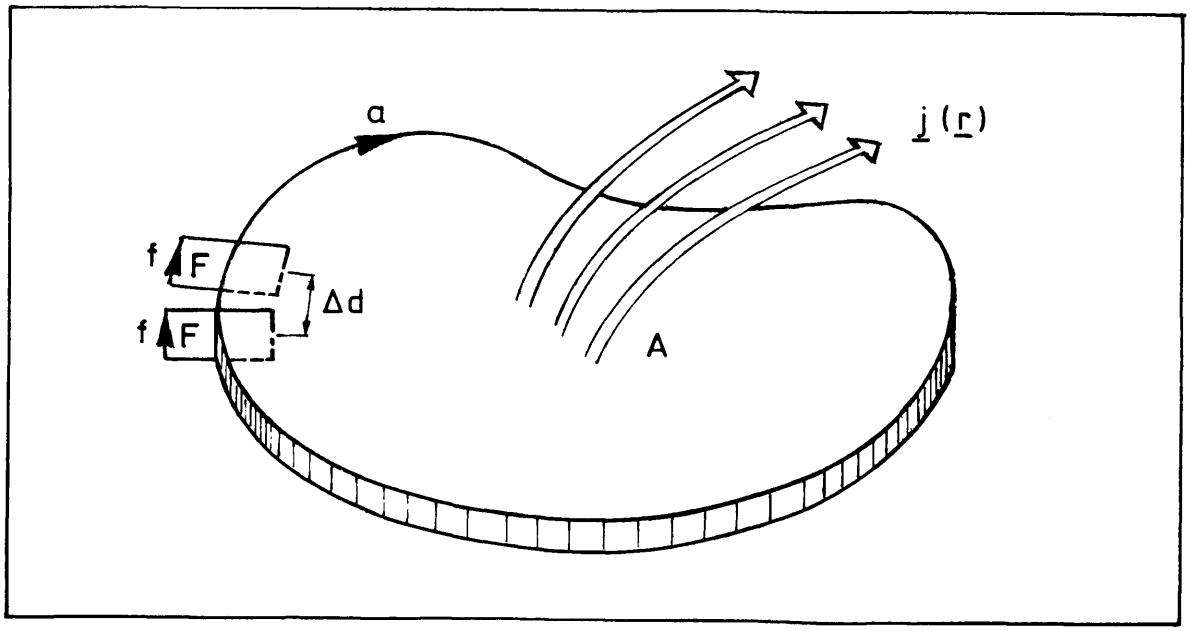

Fig. 2 Sketch of the Rogowsky principle

The induced voltage signal U_i is independent from the current distribution within the line "a" only under the following conditions:

(a) The pick-up coil is wound n-times round line "a" so that F has always the same area for all turns and is perpendicular to "a". The integral

in eq. (5) can then be split into a sum and the gain for the induced voltage of n turns is

$$U_i = F \cdot \sum_{\nu=1}^{n} \frac{d}{dt} B_{\nu\parallel} \quad , \tag{6}$$

where $B_{\nu\parallel}$ is the field component parallel to the normal vector of "F".

(b) The distance Δd between turns is constant and is small compared to magnetic field inhomogenities along the integration line "a". This leads with eq. (4) to

$$\Delta d \cdot \sum_{\nu=1}^{n} B_{\nu\parallel} = \mu\mu_o I \ . \tag{7}$$

For a coil length ℓ and uniform distances Δd, the relation is

$$\Delta d = \frac{\ell}{n} \ . \tag{8}$$

Differentiating with respect to time in eq. (7) and combined with eq. (6) yields the induced voltage

$$U_i = \mu\mu_o F \frac{n}{\ell} \cdot \frac{dI}{dt} \ , \tag{9}$$

U_i is now proportional to the time derivate of the current and the proportional factor

$$M = \mu\mu_o F \frac{n}{\ell}$$

contains only geometric parameters determining the sensitivity of the coil.

The limit is reached when the current pulse length approaches the propagation time of the signal through the coil.

3. MEASURING CIRCUIT

The induced potential U_i is transmitted by cables of impedance Z to the monitor. Fig. 3 shows the simplified circuit diagram.

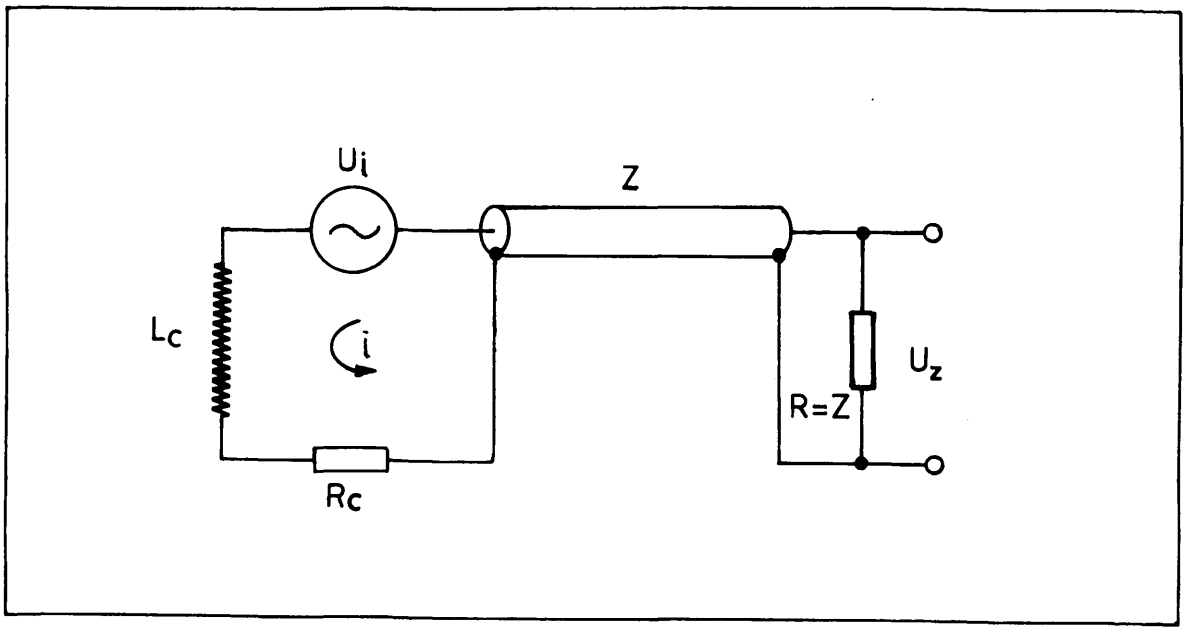

Fig. 3 Equivalent measuring circuit

The symbols used are:

U_i = induced signal,
L_c = coil inductance,
R_c = resistance of coil,
R = terminating resistor,
Z = cable impedance,
U_z = voltage on terminating resistor.

Combining the circuit equation

$$U_i = L_c \cdot \frac{di}{dt} + (R_c + R)\, i \,, \tag{10}$$

with $U_z = R \cdot i$ yields

$$U_i = \frac{L_c}{R} \frac{dU_z}{dt} + \left(\frac{R_c}{R} + 1\right) U_z \,. \tag{11}$$

As expressed by eq. (9), U_i is proportional to the time variation of the discharge current $\frac{dI}{dt}$. Therefore, two terms of the value of $\frac{L_c}{R} \cdot \frac{dU_z}{dt}$ should be considered:

(a) $$\frac{L_c}{R} \frac{dU_z}{dt} >> \left(\frac{R_c}{R} + 1\right) U_z \,. \tag{12}$$

Here the measured signal U_z is proportional to the discharge current I. The coil is self-integrating with the time constant (L_c/R).

(b) The coils developed at CERN belong to a type, where

$$\frac{L_c}{R}\frac{dU_z}{dt} \ll \left(\frac{R_c}{R} + 1\right) U_z \quad . \tag{13}$$

At this condition, U_z is proportional to $\frac{dI}{dt}$, the coil is differentiating.

To evaluate eq. (13) an harmonic approximation for U_z of

$$U_z = U_{zo} \sin \omega t \tag{14}$$

is assumed. The condition describing the upper limit for the induced frequency $\omega = \omega_{\mu\ell}$ of the discribed circuit, so that U_z is still proportional to (dI/dt), is

$$L_c \, \omega_{\mu\ell} \ll R_c + R \quad . \tag{15}$$

The resistance is mainly determined by the impedance of the cable between coil and pre-amplifier. Thus, the self-inductance of the coil must be minimized for high frequency transmission.

Rearanging eq. (15) gives

$$L_c \ll \frac{R_c + R}{\omega_{\mu\ell}} \quad . \tag{16}$$

Inserting for $R_c + R \sim 100\ \Omega$, a realistic value for shielded twisted pair signal cables and $2\pi \cdot 10^6 s^{-1}$ for $\omega_{\mu\ell}$, the maximal ringing frequency of the pulse generator yield

$$L_c \ll 1.6 \cdot 10^{-5}\ H \quad . \tag{17}$$

The required extreme low inductance of the measuring coil, together with the needed length round the plasma lens in the restricted space available between the lens cylinder and the outer conductor, i.e. a bended coil of 1 mm thickness inclusive shielding and 840 mm length, could only be achieved by using the printed circuit board technique. A coil constructed by this proceedure units the following features:

(a) Low inductance.

(b) Greatest flatness.

(c) This extreme flatness yields high flexibility, giving the possibility to wrap the coil around current conductors of any shape.

(d) Either the dI/dt and/or the integrated current signal can be measured.

(e) Excellent spatial integration over the current distribution.

(f) Selection of the output voltage by varying the circuit board thickness.

(g) The four layer technique (2 coils superimposed) brings the terminals to the same side. Voltage signals induced by flux penetration into the measuring coil are therefore suppressed.

(h) Easy reproducibility at low tolerance.

(i) Superior long-term stability.

These considerations lead to the development of the measuring coils described.

4. CONSTRUCTION OF THE COILS

The simplified coil structure is shown in fig. 4. The width of the coils was imposed by a 20 mm gap foreseen to house the coils between the strip lines and the central support of the plasma lens. Allowing for an electrostatic shielding (sect. 5) the active width of the coils was fixed to 10 mm. The distance of 10 mm between turns was selected to compensate even small current displacements in the strip lines.

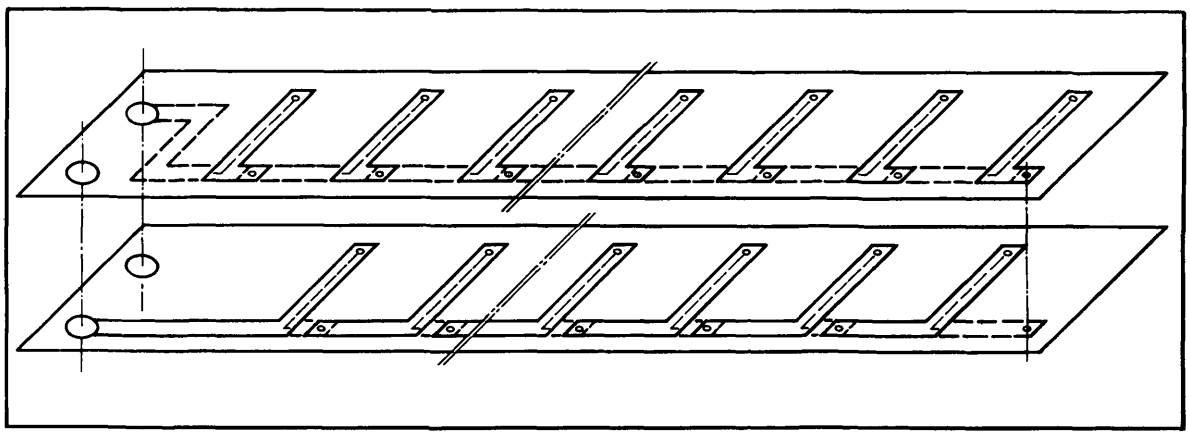

Fig. 4 The coil structure

Introducing the necessary parameters in eq. (9) for a selected output voltage of 100 V at a current rise of $5 \cdot 10^{11}$ A $\cdot$ s^{-1} and 100 cm length it follows:

$$F \cdot n \sim 1.6 \cdot 10^{-4} \text{ m}^2.$$

This yields a coil thickness of 160 µm at n = 100 turns. Based on this data, different types of coils represented in fig. 5 were constructed. The main parameters are compiled below in table 2.

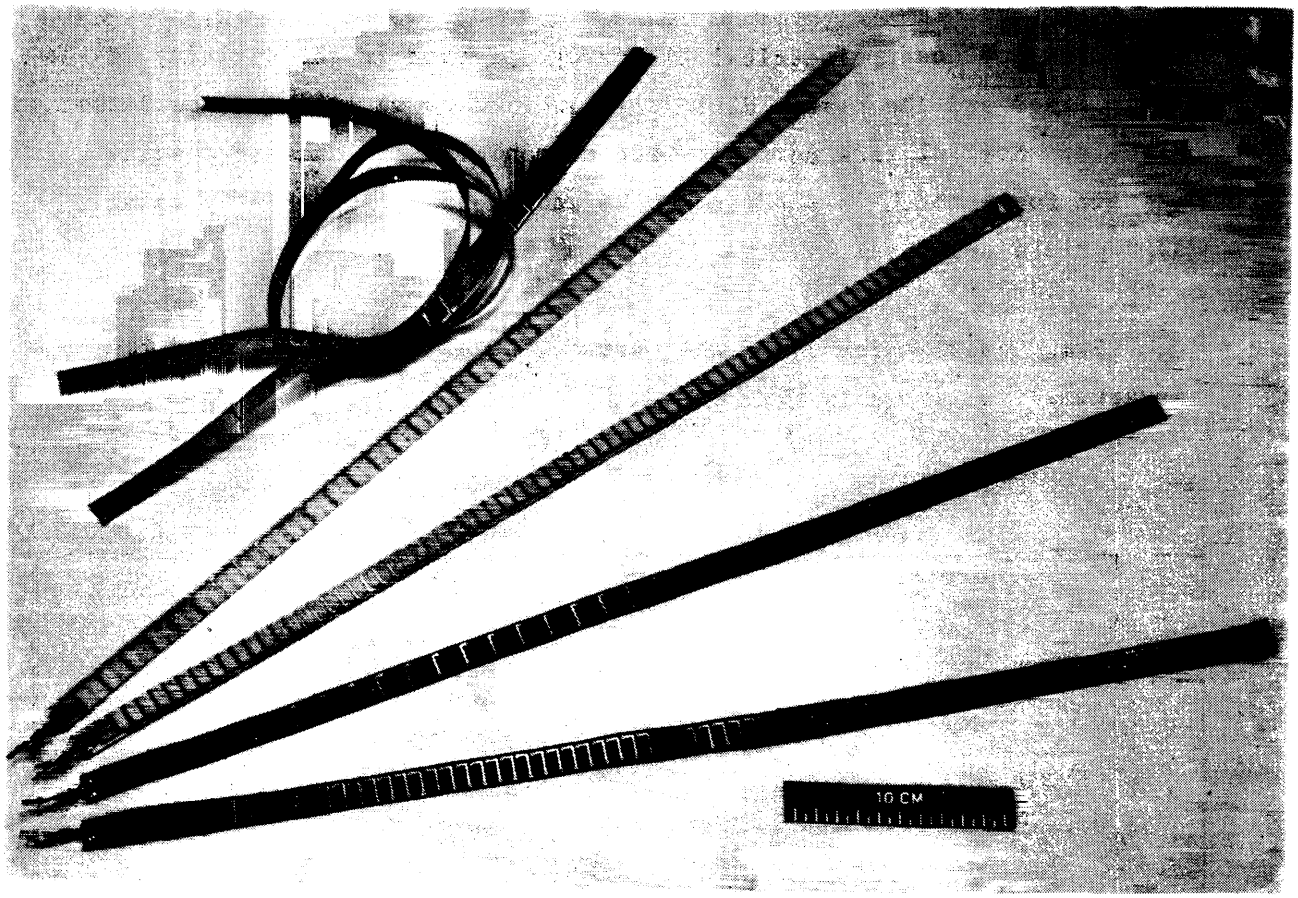

Fig. 5 Photograph of different coil types

TABLE 2 Main data of the coils

Coil No.	Number of turns (n)	Thickness (µm)	Length (mm)	Width (mm)	Winding density (cm/n)	Use
a	2 x 76	2 x 125	2 x 570	10	0.375	Strip line
b	2 x 38	2 x 125	2 x 570	10	0.75	Strip line
c	2 x 76	2 x 500	2 x 570	10	0.375	Strip line
d	2 x 38	2 x 500	2 x 570	10	0.75	Strip line
e	2 x 114	2 x 125	2 x 840	10	0.375	Lens
f	2 x 57	2 x 125	2 x 840	10	0.75	Lens

The winding density ℓ/n which determins the integration step for the spacial distributed current density was selected to be either 0.750 or 0.375 cm/n. The inductance L of the coil depends only linearly and not quadratically on the length l, and therefore on n, and is determined by the strip line geometry. For a width w and a distance d it is given by

$$\frac{L}{\ell} = \mu_o \frac{d}{w} . \qquad (18)$$

5. SHIELDING

Time dependant electrical fields are present in the vicinity of the strip lines and the plasma discharge, and induce superimposed perturbation signals. Special care must be taken to minimize the undesired noise signals for both the strip line coils and the plasma bobbin by using appropriate shielding.

Space restriction round the plasma lens allowed only a sandwich-type arrangement as shown in fig. 6.

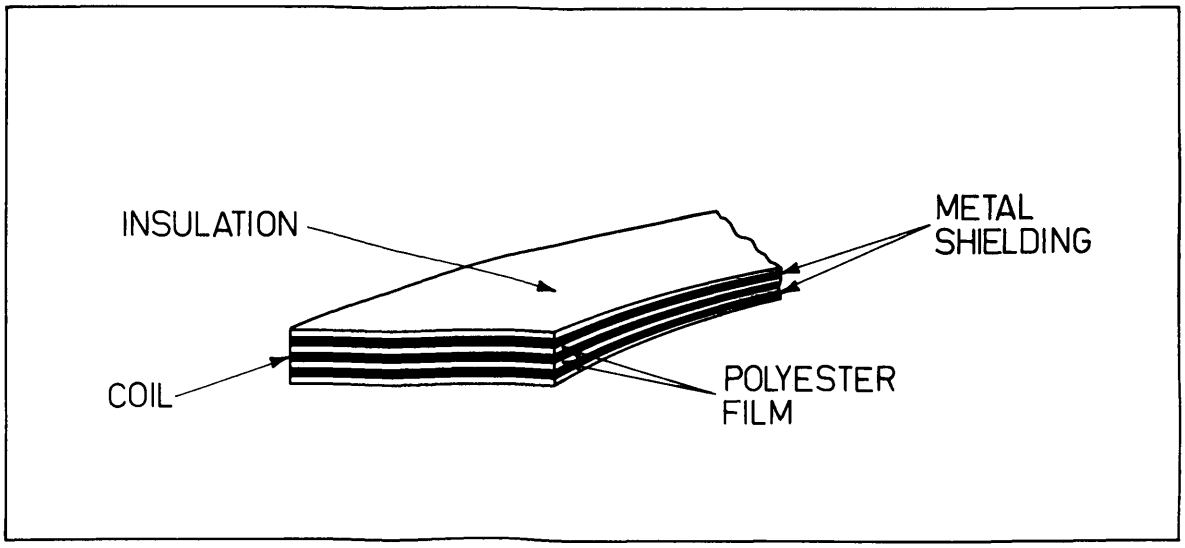

Fig. 6 Layout of an electrostatic shielding

It is obvious that the thickness of the polyester film represents a compromise between minimum capacitive coupling and maximum shielding effect. It may be worth mentioning that the earthing of the copper layers is crucial.

The space available for the strip line coils allowed to house a closed M-U shape shielding. This arrangement is shown in fig. 7.

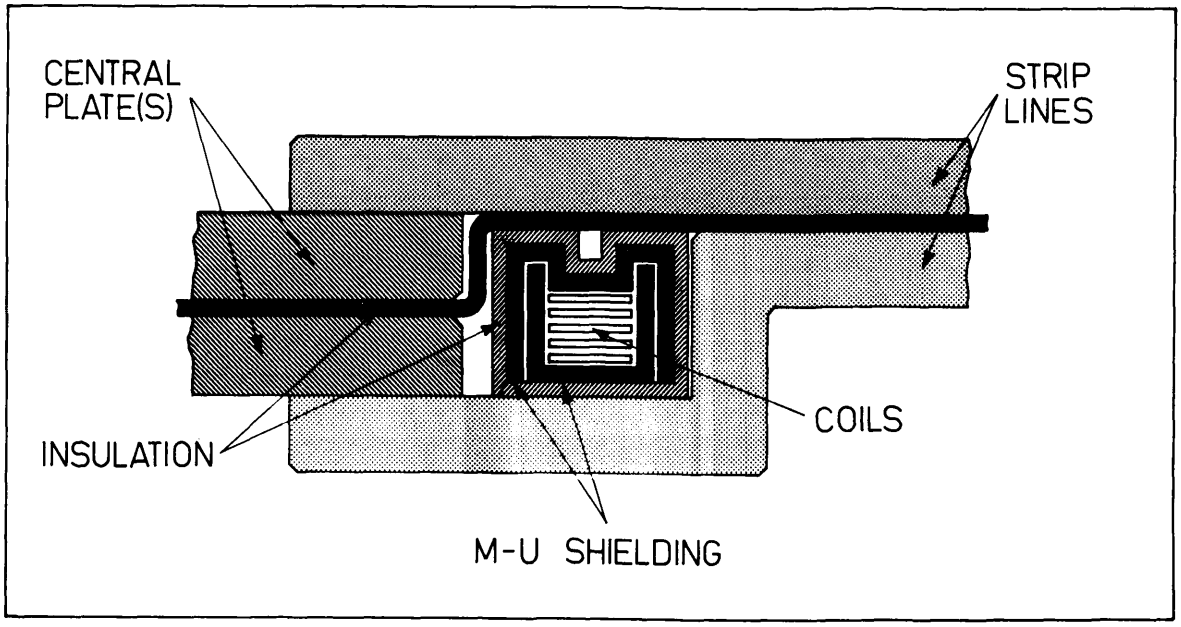

Fig. 7 Transverse cross section of coils and M-U type shielding near control plok

Several coils are accommodated in the metallic, non-magnetic, case permitting simultaneous dI/dt and $\hat{I}$ observations as well as interlock connection. The efficiency of this type of shielding is shown in fig. 8.

6. RESULTS AND MEASUREMENTS

The results of the inductance measurements up to 5 MHz are shown in fig. 9. All coils tested have values of less than 1000 nH and no resonant frequency was detected. Coil "d" was selected for the current measurements of the four strip lines and coil "f" was taken to monitor the current in the plasma lens.

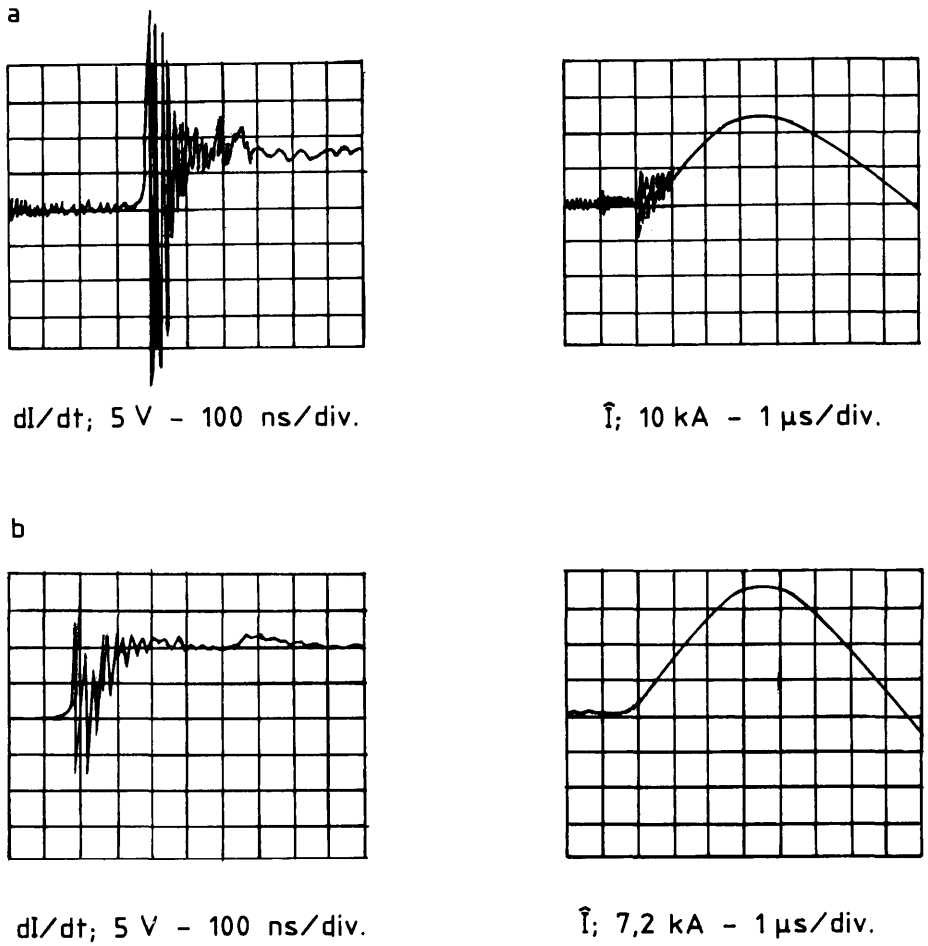

Fig. 8 Effect of shielding on noise level for: (a) Sandwich type shielding and (b) M-U type shielding

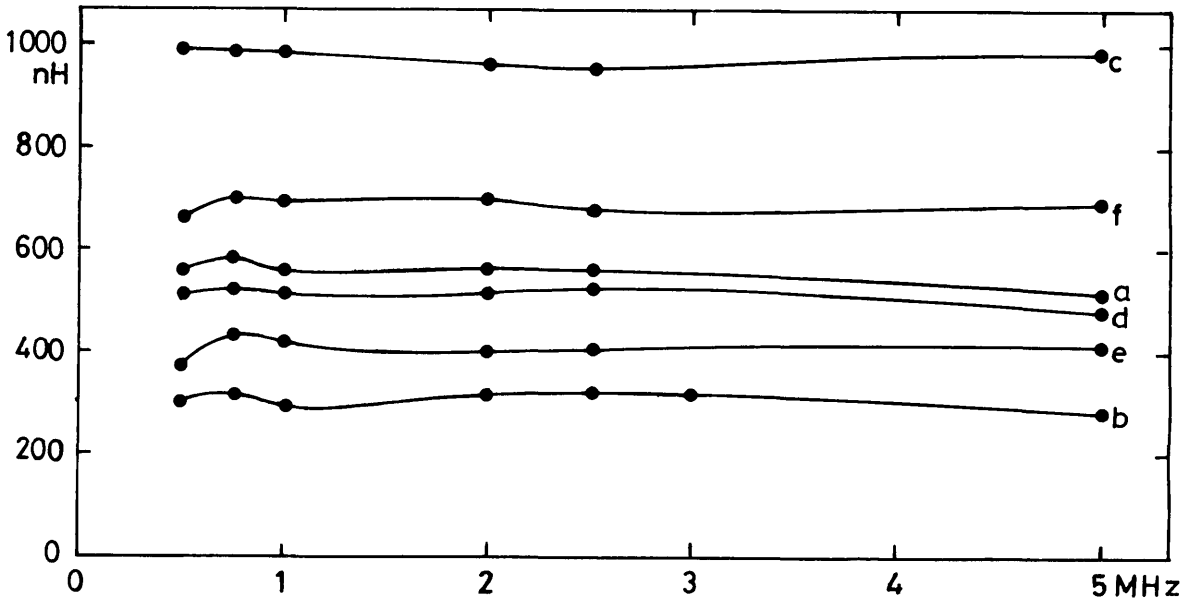

Fig. 9 Variation of self inductance versus frequency

Eq. (15) gives the limit for the upper frequency $\omega_{\mu\ell}$, where the induced voltage U_i is still proportional to the rate of change of the current dI/dt. The measured inductance L ~ 5 • 10^{-7} nH and 7 • 10^{-7} nH for coil "d" and "f" respectively is more than a factor of twenty lower than stipulated in eq. (17).

As the magnetic stray field outside the stripline proved to be negligible compared to the inner field (by a factor 40) the M-U shielded coils were inserted between the plates (fig. 7) so not really surrounding the conductor.

Two sandwich type shielded coils f surrounded the lens leading to a simultaneous I and dI/dt signal.

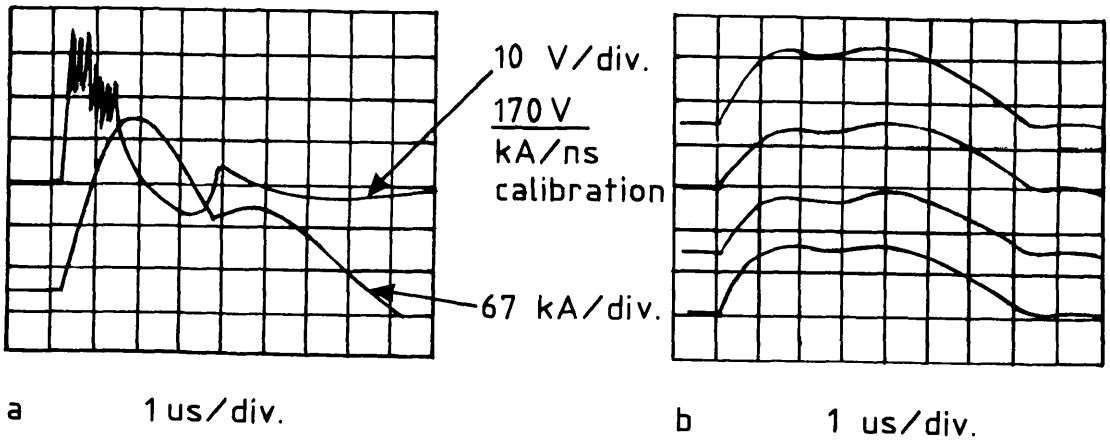

Fig. 10 Current signals of a pinched discharge: (a) ($dI/dt_{(top)}$) and $\hat{I}$; (b) simultaneous registration of the four strip line currents (4 x 100 kA)

7. CONCLUSION

The coils developed for the CERN plasma lens project proved to be a versatile tool for measuring high pulsed current signals. Calibration against a high precision, low inductive, shunt shows excellent linearity and a realistic reproduction of the pulse shape with a passive 1 ms RC integration circuit.

The common printed circuit board techniques allow to reproduce from one master print flexible, multi-purpose measuring coils of nearly any size.

For current pulses of higher frequencies, as in the application described, the self-inductance of the coils can be lowered by reducing the printed circuit thickness. In addition, eq. (9) shows that the increased dI/dt values associated with higher frequencies require a smaller geometric factor M, to reach a comparable signal amplitude. Thus, the inductance can be further reduced.

Acknowledgements

The authors wish to thank their colleagues H. Riege and V. Brückner for helpful conversations.

This work was performed as part of CERN's ACOL Project under the leadership of E. Jones from the PS Division. The encouragements of P. Lazeyras of the Experimental Physics Facilities Division is also gratefully acknowledged.

REFERENCES

[1] L. DeMenna, G. Miano, B. Autin, E. Boggasch, K. Frank and H. Riege, Plasma lens for the CERN antiproton source, Proc. of IVth Nat. Congress of Quantum Electronics and Plasma Physics, vol. 1 (1984) 273 (and CERN/PS 84-13 (AA)).

[2] E. Boggasch, H. Riege, V. Brückner, A 400 kA pulse generator with pseudo-spark switches, CERN/PS 85-30 (AA) and Proc. 5th IEEE Pulsed Power Conference, Arlington, Washington D.C., P III-36 (1985) 820-823.

[3] E. Boggasch and H. Riege, The triggering of high current pseudo-spark switches, Proc. of the XVIIth Int. Conf. on Phen. in Ionized Gases, vol. 2 (1985) 567 (and CERN/PS 85-4 (AA)).